High-frequency measurements of spin-valve films and devices (invited)

Shehzaad Kaka, John P. Nibarger, and Stephen E. Russek[a)]
National Institute of Standards and Technology, Boulder, Colorado 80305

N. A. Stutzke
Boise State University, Boise, Idaho 83725

S. L. Burkett
University of Arkansas, Fayetteville, Arkansas 72701

(Presented on 14 November 2002)

High-frequency measurements of spin-valve films and devices, made using several different measurement techniques, are presented and compared. Pulsed inductive measurements were made on sheet films and provide insight into the intrinsic dynamical properties of the component films and multilayer stacks. The damping parameter, in the completed spin-valve stack, is larger than in the constituent films. Direct time and frequency domain measurements of the dynamical response of micrometer-size spin-valve devices, made using high-bandwidth magnetoresistance techniques, showed damping parameters comparable to these measured on spin-valve sheet films. The small-angle magnetization response was also determined by high-frequency magnetic noise measurements. The damping parameters were smaller than those obtained by direct susceptibility measurements. The device-level measurements show a different dependence of the damping parameter on the easy-axis field as compared to sheet-level measurements. In addition to the uniform rotation mode, other peaks can be observed in the noise spectra that correspond to fluctuation modes arising from the micromagnetic structure. Electrical device measurements have much greater sensitivity than other high-frequency magnetic measurement techniques, which allow the direct observation of magnetization motion in submicrometer elements without averaging. This technique is used to directly examine thermally activated events and nonrepetitive dynamical motions. © *2003 American Institute of Physics.* [DOI: 10.1063/1.1558257]

I. INTRODUCTION

The high-frequency properties of magnetic multilayer thin films, being developed for giant magnetoresistive (GMR) sensor applications, have been studied by many techniques including ferromagnetic resonance (FMR), Brillouin light scattering, time-resolved magneto-optical Kerr effect, pulsed inductive techniques, and high-bandwidth magnetoresistance measurements (see Refs. 1 and 2 for recent reviews). Each technique measures slightly different properties and has its own advantages and disadvantages. Here, we present high-frequency measurements of spin-valve films and devices using pulsed inductive and high-bandwidth magnetoresistance techniques.

Pulsed inductive measurements were used to determine the dynamical properties of component films and multilayer spin-valve stacks. Pulsed inductive measurements are useful in characterizing the intrinsic dynamical properties of sheet films and allow the measurement of each layer separately or in combination and thereby measure interaction effects. Unlike FMR techniques, pulsed inductive measurements are done in the time domain and in a low field regime that more closely relates to device operating conditions.

High-bandwidth magnetoresistance measurements of micrometer dimension spin-valve devices were made to determine the response of small GMR sensors to fast magnetic field pulses and microwave radiation. The dynamical response of small devices can be further characterized, without the use of pulsed or microwave fields, by measuring thermally excited dynamical magnetization modes, which manifest themselves as voltage noise in active devices. We present magnetic susceptibility data obtained by noise measurements and compare them with direct susceptibility measurements. Noise spectroscopy is simple and can measure many nonuniform modes that cannot be seen by measurements that use long wavelength or fixed wavelength excitations.

Electrical measurements are extremely sensitive and, through the GMR effect, can measure the dynamical magnetization response of submicrometer structures over a range of motions from the linear regime to full magnetization reversal. This technique is the only method with the sensitivity to measure individual magnetization reversal events in isolated submicrometer magnetic structures. Here we present direct measurements of thermally activated switching of spin-valve elements.

The dynamical data are all analyzed in the context of the Landau–Lifshitz (LL) equation and the small angle approximations for the transverse magnetic susceptibility of a thin-film element[3]

[a)]Electronic mail: russek@boulder.nist.gov

 © 2003 American Institute of Physics

Downloaded 20 Jun 2003 to 132.163.52.130. Redistribution subject to AIP license or copyright, see http://ojps.aip.org/japo/japcr.jsp

$$\chi'(f)=(\mu_0 M_s)^2 \times\left[\frac{\mu_0^2(H_k+H_l)M_s-\frac{f^2}{\gamma'^2}}{\left(\mu_0^2(H_k+H_l)M_s-\frac{f^2}{\gamma'^2}\right)^2+\left(\frac{f}{\gamma'}\alpha\mu_0 M_s\right)^2}\right], \tag{1a}$$

$$\chi''(f)=\frac{f}{\gamma'}\alpha\mu_0 M_s \times\left[\frac{\mu_0^2 M_s^2+\frac{f^2}{\gamma'^2}}{\left(\mu_0^2(H_k+H_l)M_s-\frac{f^2}{\gamma'^2}\right)^2+\left(\frac{f}{\gamma'}\alpha\mu_0 M_s\right)^2}\right], \tag{1b}$$

where χ' and χ'' are the real and imaginary parts of the transverse susceptibility (the ratio of the hard-axis magnetization to the hard-axis field); $\gamma'=ge/4\pi m$ is the gyromagnetic ratio divided by 2π (e and m are the electron charge and mass); M_s is the saturation magnetization; H_k is the uniaxial anisotropy field, which measures the stiffness for in-plane deviations from the easy axis; H_l is the applied easy-axis or longitudinal field, and α is the Gilbert damping parameter, which is proportional to the FMR linewidth. Here we assume single-domain behavior and H_k, $H_l \ll M_s$. The susceptibility in Eq. (1) is due to uniform magnetization rotation, although the susceptibility can be generalized to include a sum over all modes of the magnetic system.

The films were sputter deposited on oxidized silicon wafers. A field of 15 mT was applied during deposition to set the pin direction and create an induced uniaxial anisotropy. The magnetic properties were measured using superconducting quantum interference device and alternating gradient magnetometers.

II. PULSED INDUCTIVE MEASUREMENTS ON SHEET FILMS

Pulsed inductive measurements were made using a pulsed inductive microwave magnetometer.[4] The pulsed inductive technique measures the induced voltage created by the time-varying magnetization that is being driven by a 60 ps rise-time step pulse generated by an underlying coplanar waveguide (CPW) (see the inset in Fig. 1). The magnetic signal, which is determined by measuring the transmitted pulse and subtracting a reference pulse taken when the magnetization is saturated, is proportional to the rate-of-change of the average magnetization component transverse to the axis of the waveguide. Measurements of the magnetization dynamics of an isolated free layer coupon (1 cm square), in response to hard-axis field pulses (H_p), are shown in Fig. 1(a) for several values of longitudinal bias field, which is applied along the easy axis of the film and along the axis of the waveguide. The measurements of the completed spin-valve stack are shown in Fig. 1(b). For the spin-valve measurements, the fixed layer and initial free layer magnetizations are oriented parallel to the axis of the waveguide and the excitation pulse is oriented transverse to this axis. The dynamical response of the isolated free layer and the completed spin valve are similar and show damped precessional relaxation characterized by a resonant frequency of 1–3 GHz and a relaxation time of 1–3 ns. The completed spin valve shows slightly lower damping times and, for both samples, the damping time increases with longitudinal bias field.

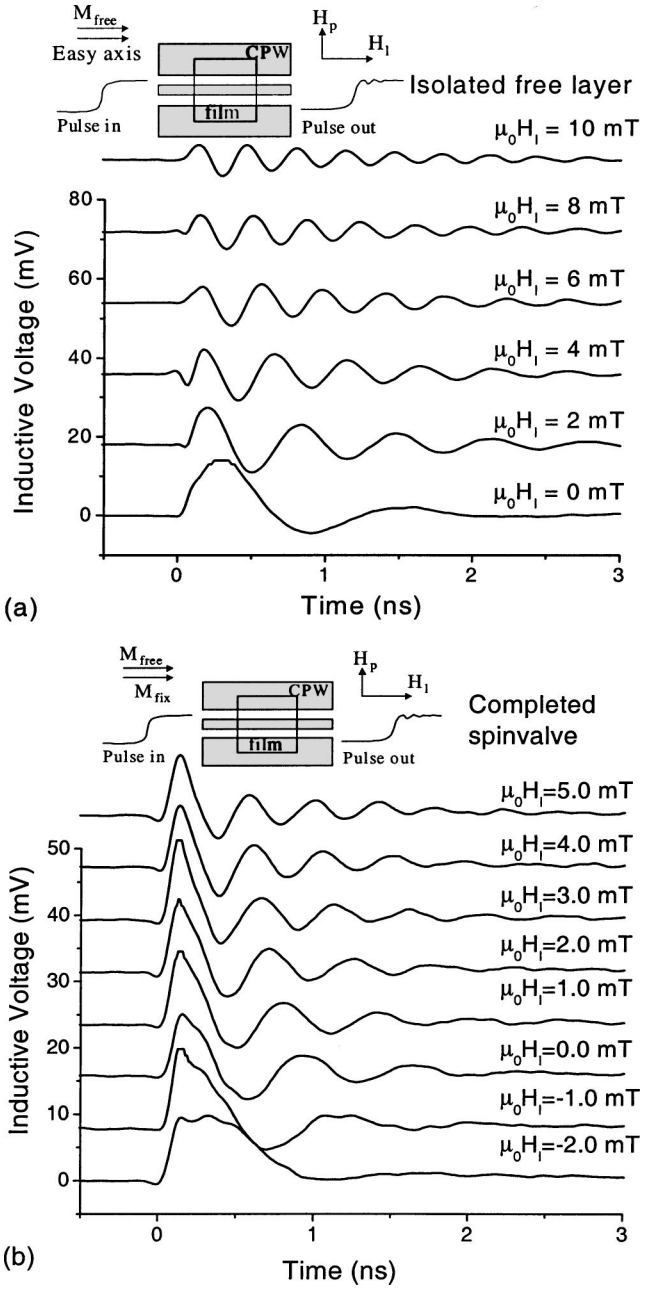

FIG. 1. (a) Pulsed inductive data for the free layer alone [Ta(5 nm)–$Ni_{0.8}Fe_{0.2}$(5 nm)–$Co_{0.9}Fe_{0.1}$(1 nm)–Cu(2.7 nm)] as a function of longitudinal field. (b) Pulsed inductive measurements of the completed spin-valve wafer. The spin-valve structure is Ta (5 nm)–$Ni_{0.8}Fe_{0.2}$(5 nm)–$Co_{0.9}Fe_{0.1}$(1 nm)–Cu(2.7 nm)–$Co_{0.9}Fe_{0.1}$(2.5 nm)–Ru(0.6 nm)–$Co_{0.9}Fe_{0.1}$(1.5 nm)–$Ir_{0.2}Mn_{0.8}$(10 nm)–Ta(5 nm). The field geometry and initial magnetization states are shown in the insets.

The measured pulse response of the spin valve is almost entirely due to the motion of the free layer since the pulsed field amplitude (~0.4 mT) is much less than the pinning field (~50 mT). The isolated free layer and the free layer in the

Downloaded 20 Jun 2003 to 132.163.52.130. Redistribution subject to AIP license or copyright, see http://ojps.aip.org/japo/japcr.jsp

completed spin valve are, however, magnetically very different. The isolated free layer has a clear uniaxial anisotropy with an easy-axis coercivity of 0.2 mT and an anisotropy field of 0.6 mT, as measured from the $M-H$ curves. The response of the free layer magnetization in the spin valve is dominated by magnetostatic coupling to the pinned layer, which arises from interfacial roughness. This coupling causes the free layer magnetization to lie along the direction of the fixed layer magnetization in zero applied field. The magnetostatic coupling field, as measured from the shift in the $M-H$ loop, was ~1.5 mT, however, the free layer did not completely reverse until 3 mT. For the negative applied fields (antiparallel to the zero-field free-layer magnetization) the spin-valve film is in a multidomain state with the regions antiparallel to the bias field contributing a low frequency response and the regions parallel to the field contributing a high-frequency response.

Figure 2(a) shows the magnitude of the Fourier transform of the measured inductive response of the spin-valve film with a 2.0 mT longitudinal bias field. The frequency-domain data are proportional to the magnitude of the transverse susceptibility[4] and shows an FMR peak at 1.8 GHz. The data are fit, using Eq. (1), with a damping parameter of $\alpha=0.023$ and $\mu_0 H_k = 2.5$ mT. The time-domain data and a curve numerically calculated from the LL equation, using the parameters taken from the frequency domain fit, are shown in Fig. 2(b). The inset shows the calculated time dependence of the transverse magnetization. All of the data in Fig. 1 were similarly fit.

The results of fitting to the frequency domain data for the isolated free layer and the completed spin valve are shown in Figs. 3(a) and 3(b). The resonant frequency is well fit using the Kittel equation $f_r \cong \gamma' \mu_0 \sqrt{(H_k+H_l)M_s}$ with constant anisotropy fields of $\mu_0 H_k = 0.8$ and 2.31 mT for the isolated free layer and completed spin valve, respectively. The values of the Gilbert damping parameter α, determined from the frequency-domain fits, are also shown in Figs. 3(a) and 3(b) for the isolated free layer and the completed spin valve stack, respectively. The values of α for the isolated free layer decrease from 0.02 at 0.0 mT bias field to 0.01 at 10.0 mT bias field. The values for the completed spin valve decrease from 0.03 at -2.0 mT bias field to 0.02 at 6.0 mT bias field. This decrease in α is consistent with that observed in sheet films of $Ni_{0.8}Fe_{0.2}$.[4] The interpretation of the fitted damping parameter for the completed spin valve, for bias fields below 0 mT, is unclear since the single-domain model is not valid. In the single-domain regime, α is fairly constant. It is expected that the spin-valve the stack will show larger damping than the isolated free layer since additional energy and angular momentum loss mechanisms can be introduced. The magnetostatic coupling of the free layer to the fixed layer will lead to spin-wave generation in the fixed layer when the free layer rotates, which is an additional energy loss mechanism that is not present in the isolated free layer. Other additional loss mechanisms are also predicted.

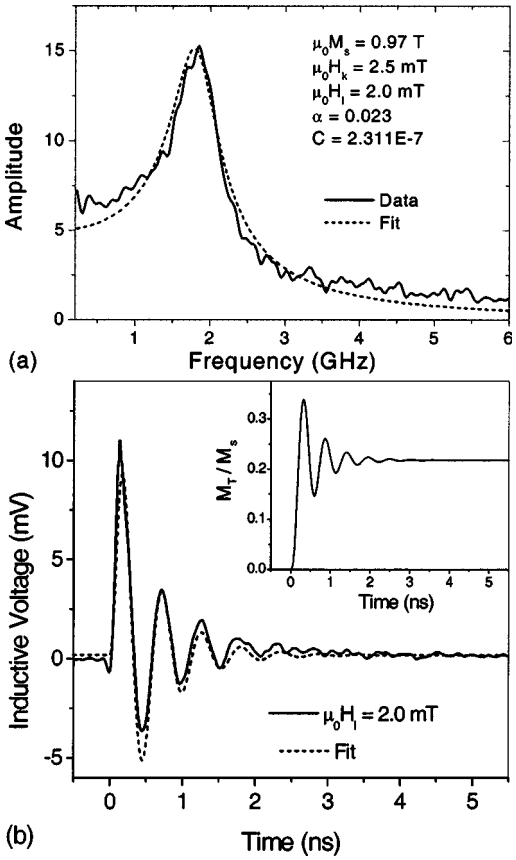

FIG. 2. (a) Fourier transform of the time domain data for the completed spin-valve film with a 2.0 mT longitudinal bias field and a fit to the transverse susceptibility calculated from Eq. (1). The fit allows H_k, α, and an overall scale constant C, to vary; M_s and H_1 are determined experimentally. (b) Pulsed inductive data for the spin-valve film for 2.0 mT longitudinal field, which is proportional to the time derivative of the transverse magnetization, and calculated response using a single domain model with the parameters determined by the fit in (a). The inset shows the calculated time-dependent transverse magnetization.

III. HIGH-BANDWIDTH MAGNETORESISTANCE MEASUREMENTS OF DEVICES

High-bandwidth magnetoresistance measurements of patterned spin-valve elements can be made in both the time and frequency domain.[6] The voltage signal from a spin-valve device, with a constant bias current, is proportional to the device resistance, which depends on the device magnetization state. The resistance change in a spin valve is proportional to the cosine of the angle between the free and fixed layer or, alternatively, the component of the free layer magnetization along the direction of the fixed layer. The dominant anisotropy energy in patterned elements is due to magnetostatic shape anisotropy, which causes the easy axis of the free layer to be along the long dimension of the device. For the devices studied here, the anisotropy fields, as measured from hard-axis magnetoresistance curves, varied between 8 and 12 mT.

The magnetoresistive response for a spin-valve device, being driven by a hard-axis step pulse produced by an overlying microstrip line, is shown in Fig. 4(a). The step pulse is similar to that used in the pulsed inductive measurements but now the waveguide is much smaller (4 μm) and hence the magnetic field pulse is larger. The hard-axis pulse amplitude

Downloaded 20 Jun 2003 to 132.163.52.130. Redistribution subject to AIP license or copyright, see http://ojps.aip.org/japo/japcr.jsp

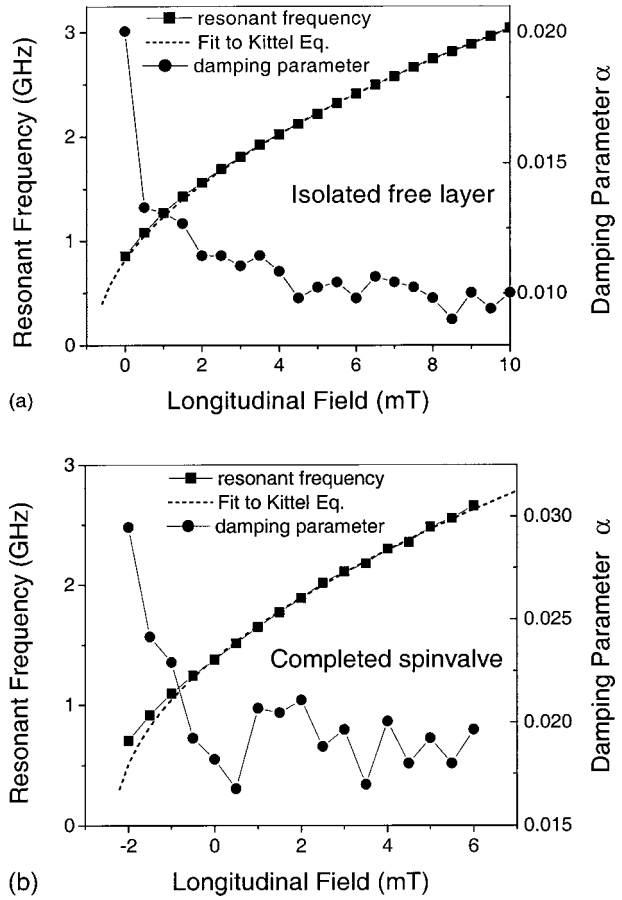

FIG. 3. Results of fitting the frequency-domain pulsed inductive data to a single domain model. (a) The resonant frequencies and the damping parameters for the isolated free layer as a function of longitudinal bias field. The resonant frequency data is fit using the Kittel equation with $\mu_0 M_s = 0.97$ T, $\mu_0 H_k = 7.9$ mT, and $g = 2.12$. (b) The resonant frequencies and the damping parameters for the completed spin-valve film. The resonant frequency data is fit using the Kittel equation with $\mu_0 M_s = 0.97$ T, $\mu_0 H_k = 23.1$ mT, and $g = 2.09$.

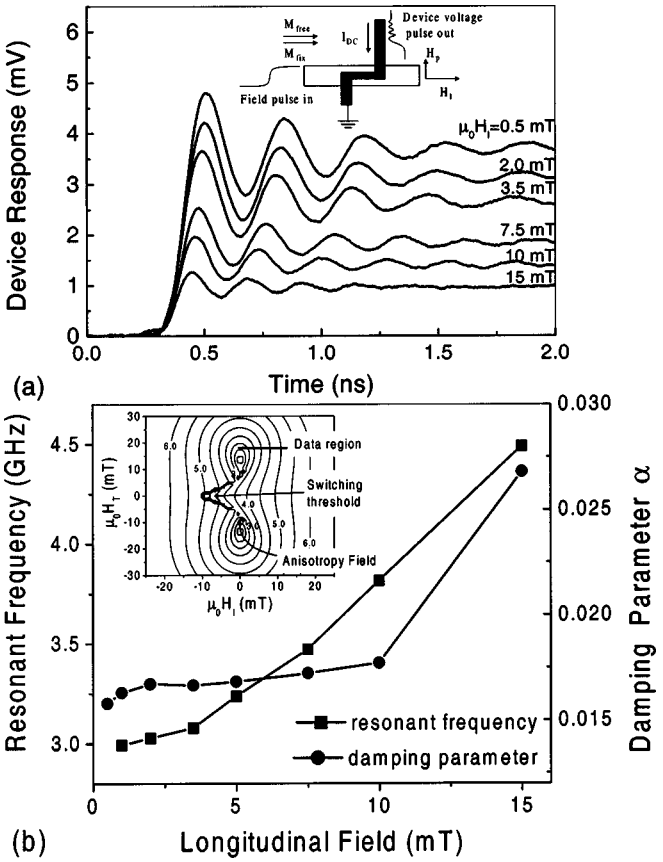

FIG. 4. (a) Magnetoresistive response of a spin-valve device to a transverse step pulse. The layer structure is Ta 5.0 nm–$Ni_{0.8}Fe_{0.2}$1.5 nm–Co 1.0 nm–Cu 3.0 nm–Co 2.0 nm–Ru 0.6 nm–Co 1.5 nm–FeMn 10nm–Ta 5.0 nm and the device dimensions are 0.8×4.8 μm^2. The field pulse is provided by a microstrip line above the device as shown in the inset. (b) Resonant frequencies and damping parameter determined from fitting the data. The inset shows a calculated contour plot of the resonant frequencies (in GHz) as a function of longitudinal and transverse field. The horizontal line shows the region of field space sampled by the data.

is approximately 20 mT. The spin valve had the fixed layer pinned along the easy axis of the free layer. This configuration, which measures the easy-axis magnetization component, is useful for characterizing high-angle rotations and is not sensitive to small-angle rotations. The data are similar to that shown in Fig. 1 except that the signal is now proportional to the easy-axis magnetization, not the derivative of the hard-axis magnetization, and the dimension of the samples are on the order of micrometers, not millimeters.

The data can be fit with a single-domain model to obtain the resonant frequencies and the damping parameters. The results of the fits are shown in Fig. 4(b). The resonant frequencies do not show the same dependence on the longitudinal bias fields as in the pulsed inductive measurements because the perpendicular pulse amplitude is now large compared to the longitudinal bias field and anisotropy field. The inset in Fig. 4(b) shows a contour plot of the resonant frequencies calculated using a single-domain model and indicates the region where these measurements were taken. The single-domain calculations give larger values of the resonant frequency but the calculated resonant frequencies show the same qualitative field dependence as the data. The range of α is similar to what is seen in the pulsed inductive data except that now there is an increase in α at larger bias fields.

Direct measurements of the transverse susceptibility of a spin-valve device can be made by driving the device with microwave magnetic fields and detecting the signal with a network analyzer.[5] Frequency-domain susceptibility measurements are shown in Fig. 5(a). In this case, the fixed layer was pinned perpendicular to the free layer and the magnetoresistance measurements are sensitive to small angle oscillations. Also shown in Fig. 5(a) are fits to the curves using Eq. (1). While both the real and imaginary parts of the susceptibility are measured, there is some ambiguity in determining the phase of the measured response relative to the drive field, which leads to ambiguity in separating real and imaginary parts. It is, therefore, easier to fit the magnitude of the susceptibility. The resonant frequencies and damping parameters are shown in Fig. 5(b). The microwave excitation field is small ($\sim$2 mT) and the fit to the Kittel equation is reasonable, although not as good as for the sheet level measurements. The overall range of α is consistent with the wafer-level measurements, but again the field dependence shows a different behavior than the sheet-level measurements. After an initial decrease, α shows a peak at a longi-

Downloaded 20 Jun 2003 to 132.163.52.130. Redistribution subject to AIP license or copyright, see http://ojps.aip.org/japo/japcr.jsp

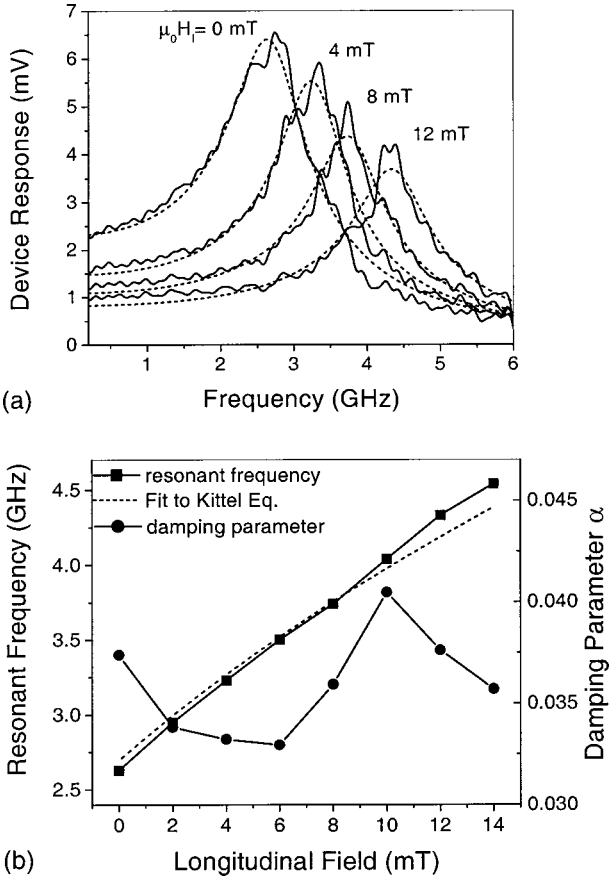

FIG. 5. (a) Direct frequency-domain measurements of the transverse susceptibility in a 0.8×4.8 μm^2 spin valve. The layer structure was Ta 5.0 nm–$Ni_{0.8}Fe_{0.2}$ 5.0 nm–Co 1.0 nm–Cu 3.0 nm–Co 2.0 nm–Ru 0.6 nm–Co 1.5 nm–FeMn 10 nm–Ta 5.0 nm. (b) The resonant frequencies and the damping parameters determined from fitting the data in (a). The resonant frequency data is fit using the Kittel equation with $\mu_0 M_s = 0.97$ T, $\mu_0 H_k = 8.5$ mT, and $g = 2.12$.

tudinal field value of 10 mT. It is expected that, due to the large nonuniform magnetostatic fields present in the device, there may be some micromagnetic structure (deviations from uniform magnetization). The peak in the damping may, therefore, be correlated with a change in the micromagnetic state of the device.

IV. HIGH-FREQUENCY MAGNETIC NOISE IN DEVICES

Instead of driving GMR devices with fast magnetic field pulses or microwave radiation, it is possible to monitor the device response to intrinsic thermal fluctuations. If the device is small enough, the thermal magnetization fluctuations, which scale inversely with the device volume, can be detected as voltage noise. The magnetic noise spectrum is determined by measuring the voltage noise from a device in an active state and subtracting the voltage noise when the magnetization is saturated with a large hard-axis field. The fluctuation-dissipation theorem relates the thermal fluctuations of the magnetization to the imaginary part of the magnetic susceptibility.[7,8] The observed magnetic noise spectrum, measured in volts per root Hertz, is proportional to the square root of the imaginary susceptibility divided by the frequency:

$$V_n(f) = I\Delta R \sqrt{\frac{k_B T}{2\pi f \mu_0 M_s^2 V} \chi_t''(f)}, \tag{2}$$

where I is the applied current, ΔR is the change in device resistance from the parallel to the antiparallel state, V is the device volume, and T is the device temperature.

Figure 6(a) shows the noise spectra, for various longitudinal bias fields, from a spin-valve device fabricated on the same wafer used for the pulsed inductive measurements shown in Fig. 1. The data are very similar to the susceptibility data shown in Fig. 5(a) and can be fit using Eqs. (1) and (2) (see Ref. 9 for details of the fitting process). The results of the fitting are shown in Fig. 6(b). The measured resonant frequency agrees reasonably well with the Kittel formula, as expected, since the deviations from the easy axis are quite small. The calculated rms variation of the magnetization angle of these devices, at room temperature, is $\sim 0.5°$. The damping parameter shows a peak, qualitatively similar to the damping behavior measured by susceptibility measurements, although the peak occurs at smaller bias fields. The overall magnitude of α is smaller than that obtained either by sheet-level pulsed inductive measurements or device-level magnetoresistance measurements. This may be correlated with the fact that the thermal fluctuation fields, and hence the magnetization motions, are smaller than the drive fields and magnetization motions used in the other measurements.

In some devices, with small aspect ratios, additional low-frequency peaks can be observed in the noise spectra as shown in Fig. 7. These peaks have resonant frequencies that do not vary regularly with applied field and tend to vanish at large longitudinal bias fields. This suggests that the peaks are due to micromagnetic structure (nonuniform magnetization) and may be due to domain-wall motion rather than a standard magnetostatic mode. These additional peaks correlate with Barkhausen noise seen in the low-frequency MR response.

V. THERMALLY ASSISTED SWITCHING IN BISTABLE DEVICES

The high-frequency measurements reported in the previous sections all rely on averaging the magnetic response over many identical events, therefore do not represent the true dynamical response of the magnetic device since random motions, due to thermal fluctuations are averaged out. Thermal fluctuations can be measured in the time domain using high-bandwidth single-shot magnetoresistance techniques. The most dramatic thermally activated event is the reversal of the magnetization between two easy-axis states. Several thermally activated reversal events in a 0.8×4.8 μm^2 spin-valve device are shown in Fig. 8. Here, the spin-valve fixed layer is pinned along the free-layer easy axis and the magnetoresistance signal is proportional to the free-layer easy-axis magnetization, similar to the device configuration shown in Fig. 3. A short rise-time pulse, oriented antiparallel to the initial free layer magnetization are with magnitude just below the quasistatic switching threshold, is applied, and the magnetization is monitored until a thermally activated event causes the magnetization to reverse. The data are taken on a digitizing oscilloscope with a 1.5 GHz bandwidth. Unlike

Downloaded 20 Jun 2003 to 132.163.52.130. Redistribution subject to AIP license or copyright, see http://ojps.aip.org/japo/japcr.jsp

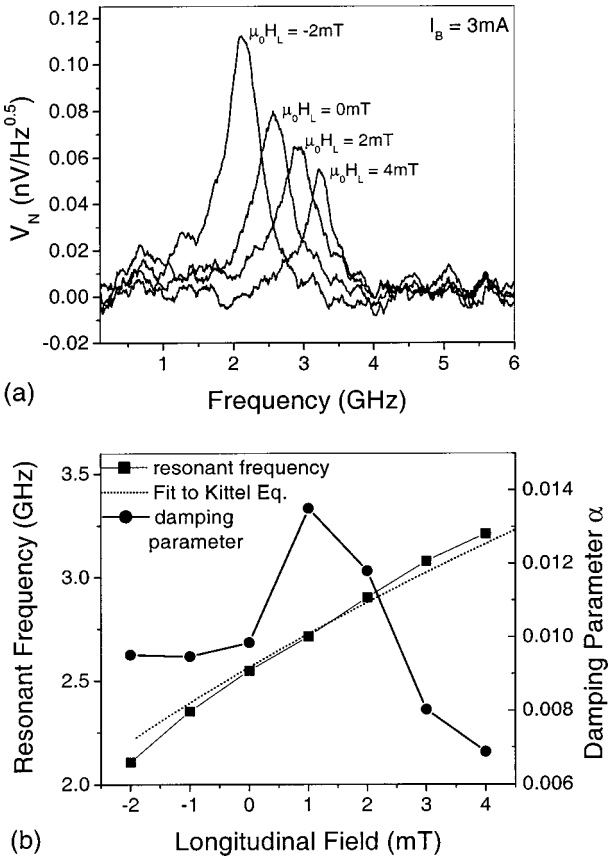

FIG. 6. (a) High-frequency magnetic noise spectra from a 1×3 μm^2 spin-valve device for a series of longitudinal bias fields (taken from Ref. 8). The noise spectra were taken at room temperature with an applied current of 3 mA. The device is fabricated from the same wafer described in Fig. 1. (b) The resonant frequencies and damping parameters determined by single domain fits to the data in (a). The resonant frequency data is fit using the Kittel equation with $\mu_0 M_s = 0.97$ T, $\mu_0 H_k = 7.7$ mT, and $g = 2.12$.

previous studies,[10] the data presented here have sufficient bandwidth to measure the stochastic motion of the magnetization in response to thermal fluctuations. Following the application of the field pulse, the switching wave forms show small steps in the magnetoresistance before the complete switch occurs. More work needs to be done to separate out the thermal magnetization motion from the system noise to conclusively identify the precursor thermal events that initiate the magnetization reversals shown in Fig. 8. However, it is clear that direct measurement of thermally induced magnetization motion is possible and is a very important component of magnetization dynamics in small GMR devices.

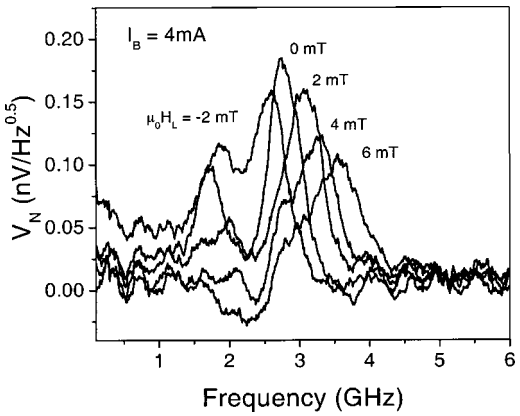

FIG. 7. High-frequency magnetic noise spectra taken on a 0.8×1.6 μm^2 spin-valve device for a series of longitudinal bias fields showing additional low frequency peaks.

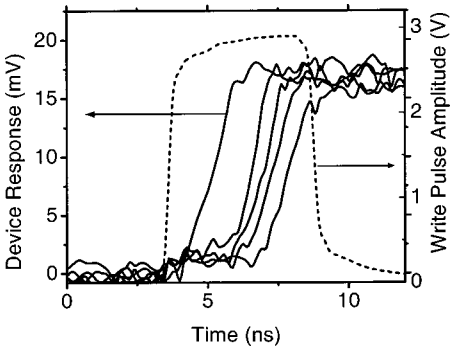

FIG. 8. Magnetoresistive response of a spin valve showing thermally activated switching between easy axis states. The magnetic field pulse, oriented antiparallel to the initial magnetization state, is shown (dotted line) along with four magnetoresistive response curves (solid lines). All four of the response curves shown are obtained for nominally identical starting states and field pulses. There is a variable dwell time for the switching to occur and there is an indication of precursor events that initiate the magnetization reversals.

VI. SUMMARY

The high-frequency response of GMR multilayer films can be measured by several methods at the wafer and device levels. The free-layer magnetization in completed spin-valve structures shows larger damping than the isolated free-layer magnetization. The noise spectra give slightly smaller values of the damping parameters than the pulsed inductive or device susceptibility measurements. The device-level measurements show more structure in the damping parameter as a function of longitudinal bias field that likely indicates there is micromagnetic structure in the device that changes with applied field. The effect of micromagnetic structure shows up clearly in devices with small aspect ratios as additional peaks in the magnetic noise spectra. Finally, real time measurements of device magnetoresistance can be used to measure thermal magnetization fluctuations and the stochastic magnetization motion that leads to irreversible events such as magnetization reversal.

ACKNOWLEDGMENTS

The authors acknowledge the support of the NIST Nanotechnology Initiative and the DARPA Spintronics Program.

[1] *The Physics of Ultra High Density Recording*, edited by M. L. Plumer, J. Van Ek, and D. Weller (Springer, Berlin, 2001).
[2] *Spin Dynamics in Confined Magnetic Structures I*, edited by B. Hillebrands and K. Ounadjela (Springer, Berlin, 2002).
[3] J. Huijbregtse, F. Roozeboom, J. Sietsma, J. Donkers, T. Kuiper, and E. van de Riet, J. Appl. Phys. **83**, 1569 (1998).
[4] T. J. Silva, C. S. Lee, T. M. Crawford, and C. T. Rogers, J. Appl. Phys. **85**, 7849 (1999).
[5] R. Urban G. Woltersdorf, and B. Heinrich, Phys. Rev. Lett. **87**, 217204 (2001).
[6] S. Russek and S. Kaka, IEEE Trans. Magn. **36**, 2560 (2000).
[7] N. Smith and P. Arnett, Appl. Phys. Lett. **78**, 1448 (2001).
[8] N. Smith, J. Appl. Phys. **90**, 5768 (2001).
[9] N. Stutzke, S. L. Burkett, and S. E. Russek, Appl. Phys. Lett. **81**, 91 (2002).
[10] N. D. Rizzo, M. DeHerrera, J. Janesky, B. Engel, J. Slaughter, and S. Tehrani, Appl. Phys. Lett. **80**, 2335 (2002).

Downloaded 20 Jun 2003 to 132.163.52.130. Redistribution subject to AIP license or copyright, see http://ojps.aip.org/japo/japcr.jsp